

EXPERIMENTS MANIFEST ELECTROMAGNETIC RADIATION FROM VARIEDLY ACCELERATING NEUTRAL BODIES AS PREDICTED BY YARMAN'S APPROACH, WHICH ALSO EXPLAINS SONOLUMINESCENCE

Tolga Yarman,¹ Ozan Yarman,² Can Yeşilyurt,³ Metin Arik,⁴
Alexander Kholmetskii,⁵ Sinan Bugu⁶

- | | |
|--|----------------------------------|
| ¹ Okan University, Istanbul, Turkey | (tolgayarman@gmail.com) |
| ² Istanbul University, Istanbul, Turkey | (ozanyarman@ozanyarman.com) |
| ³ National University of Singapore, Singapore | (ismail.can.yesilyurt@gmail.com) |
| ⁴ Bogazici University, Istanbul, Turkey | (metin.arik@boun.edu.tr) |
| ⁵ Belarus State University, Minsk, Belarus | (alkholmetskii@gmail.com) |
| ⁶ Istanbul University, Istanbul, Turkey | (sinanbugu@gmail.com) |

ABSTRACT

A series of experiments have manifested the prediction made by Yarman's Approach (YA), where neutral bodies are posited to emit electromagnetic radiation due only to changes in the rate of acceleration. Yarman et al. similarly assert that, electric charges too should radiate via the same mechanism. Hence, according to YA, neutral and charged bodies shall produce emissions in both rotational and translational non-constant acceleration scenarios. We anticipate radiation to follow a quantitatively small loss of rest mass on account of the object getting bound to its accelerational field, which is a requirement of the law of energy conservation embodying the mass-energy equivalence of the Special Theory of Relativity (STR) under the framework of YA. For a circular motion with associated variance in angular acceleration, the radiation frequency will be identical to instantaneous revolutions per second. We report herein the outcome of three experiments aimed to test the aforementioned hypothesis of YA. In our first experiment, we used a pneumatic dental drill to achieve angular velocities of up to 400,000 rpm; where, in accordance with the predictions of our model, emissions in the ULF-VLF range up to 6.5 kHz was measured. In a second experiment, colliding two empty gas cylinders once more demonstrated the emergence of electromagnetic radiation within the expected range, as a consequence of momentum gain surge from their impact points. In the third experiment, a set of steel strings under stereotypically high tension of a grand piano again irradiated in the expected frequency range when excited through forceful hammering by the keyboard mechanism, which is indicative of variegated acceleration of perturbed sections of the strings. A common feature of these experiments was the discovery that, the frequency of the electromagnetic radiation turned out to be the same as the sound frequency that had been issued to the surrounding air. We discuss our findings and possible implications, such as the one pertaining to a rigorous explanation of sonoluminescence, in this manuscript.

Keywords: Yarman's Approach (YA), YARK, special relativity, general relativity, acceleration, momentum gain, rotation, rest-mass, electromagnetic radiation, sonoluminescence, acoustic, pitch analysis, earthquake.

1. INTRODUCTION

Electromagnetic radiation from neutral bodies had been studied in quite a few extreme cases. One such case involves neutral beams of hydrogen isotopes crossing the interface between dielectric media.¹ Another is the occurrence of coherent radiation in the extremely high frequency range when neutral molecules move above a grating.² That being so, we encountered no suitable examples in the literature relevant to the topic – seeing as, the studies in question actually involve radiation from a process of commonplace excitation till a return to the ground state.

From whichever side one chooses to look at it, our paper is likely the first incident report concerning the measurement of radiation from electrically neutral macroscopic entities; where, any classical excitation or ionization of constituent atoms and molecules must be entirely ruled out.

We have already discussed in a previous publication,³ how a neutral rotating object that exhibits a change in the rate of acceleration is expected to emit radiation as a direct result of the energy conservation law within the framework of Yarman's Approach (YA). We anticipate electromagnetic radiation to follow a quantitatively small loss of rest mass due to an object getting bound to its accelerational field; which is imposed by the law of energy conservation embodying the mass-energy equivalence of the Special Theory of Relativity (STR) under the cast of YA.

Essential elements of Yarman's Approach can be found in concomitant references.^{4,5,6,7,8,9,10,11,12,13,14,15,16} Let it be stated that, the first co-author's original framework was advanced further with the involvement and support of his colleagues, and was later on called "YARK" – from the initials of Yarman-Arik-Kholmetskii – in order to designate the long-lasting collaboration in this field between said authors.^{17,18,19,20,21,22,23,24,25,26,27,28,29, 30,31,32}

Hence, in Yarman's Approach, when an entity gets bound to any attractor, it undergoes a rest mass decrease owing to the law of energy conservation embodying the mass & energy equivalence of STR. This rest mass deficit ought to be ejected in the form of radiation as the object binds itself to the source of attraction. Contrastingly, the process of deceleration would entail that, the object (*e.g.*, in the case of rotation) replenishes the rest mass it had previously discarded through energy absorption from its immediate agent of contact (*e.g.*, through air friction). This procedure is fully explained by Yarman et al. in the references provided above.

Let us emphasize, at this point, our theoretical model has been in the making since several years to address a variety of far-reaching topics, with positive outcomes receiving ever-increasing attention from the scientific community.

We may now elaborate on our earlier work regarding radiation from neutral bodies [3]. While the initial focus of our preceding paper was the ideal case of a frictionless environment – *where a rotating object is expected to radiate only during the increase of its angular acceleration*, emission of radiation even in non-isolated setups that exhibit seemingly constant (or more precisely, imperceptibly and unpreventably wavering) acceleration, or yet, hard-braking deceleration, had also been briefly explored under ref. 3.

Yarman's Approach henceforth accounts for "routine anomalies" which one would naturally encounter due to run-of-the-mill hindrances and imperfections when pursuing an experiment outside of perfect vacuum.

Be that as it may, a cornerstone feature of YA happens to be that, the frequency ν (in *hertz*) of the predicted radiation due to rotation becomes numerically equivalent to the angular velocity ω (in *rad/sec*) divided by 2π ; *i.e.*

$$\nu = \frac{\omega}{2\pi} . \quad (1)$$

What Eq. (1) signifies is, the number of turns per second achieved by the rotating object also happens to be the expected radiation frequency, or vice versa [3].

For completeness, a short synopsis on YA will be presented in Section 2 below. In the entry to Section 3, tools and methods used in three experiments for the verification of the hypothesis of YA are described. Sub-section 3.1 details the results of our first and most recent experiment, where we held close to a specially constructed loop antenna a pneumatic dental drill driven solely by a powered-down air compressor (eliminating thereby any risk of electrical interference); which clearly manifested the reception of electromagnetic radiation in the course of varying the rate of rotational acceleration of the spinning bur. In Sub-section 3.2, we elaborate on our earlier second experiment, which involved the head-on collision of two empty gas cylinders, that revealed once again radiation ensuing from neutral bodies. In Sub-section 3.3, we carry to our readers' attention the outcome of our third and earliest experiment, which shows electromagnetic emission when steel strings of a grand piano are excited through the hammer action of its keyboard. All our experiments have been carried out under ordinary atmospheric pressure and temperature.

Our findings and possible implications – such as that pertaining to an answer to the controversy on sonoluminescence, and also a preemptive method for detecting earthquakes before they strike, aside from a polyphonic score transcription benefit to the music industry without recourse to conventional pitch analysis techniques – shall be the undertaking of Section 4.

2. BASIC ELEMENTS OF YARMAN'S APPROACH

Yarman's Approach (YA) principally differs from the General Theory of Relativity (GTR) in its philosophical foundations. In contrast to the purely metric layout of GTR, Yarman's theory is built directly on the basis of the law of energy conservation appertaining to interaction between masses. For a test object moving in the presence of a gravity source, the overall relativistic energy E is postulated in the form of

$$E = \gamma m_{0\infty} c^2 \left(1 - E_B / m_{0\infty} c^2\right), \quad (2)$$

where c is the speed of light in empty space, $m_{0\infty}$ is the rest mass of the given object measured at infinitely far away from everything else, γ is the Lorentz coefficient associated with the motion of the object at hand, and E_B is the “static binding energy” – *i.e.*, the energy one has to furnish to the object, were it at rest at the given location, to carry it quasi-statically to an infinite distance.

This equation is, in effect, none other than the direct expression of the law of energy conservation under the framework of YA.

Eq. (2) tells us that, the rest mass (or the same, *rest energy*, were c taken unity) of the object $m_{0\infty}$ is decreased in a gravitational environment by the value of the static binding energy E_B . In other words, gravitational energy in YA is considered to be localized inside the gravitating object rather than being distributed across “a field of interaction” between masses.

The next essential feature of YA is the closed relationship between the quantities “energy”, “mass”, and “time rate”; which allows us to assert that rest mass variation of a test particle by the related change in its static binding energy affects – via the associated quantum mechanical description – the time rate for the particle (*i.e.*, through the modification taking place in the rest mass parameter of the corresponding – *whichever is appropriate* – Schrödinger or Dirac description) [4,5,8,11,12]. The variation of the time rate simultaneously induces a conjoint transformation of spatial intervals as observed from the synchronous reference frame co-moving with the particle. However, no *warping influence* by the host massive body on space-time geometry is assumed [25].

As shown in [25], this approach allows the elimination of ambiguities that would otherwise arise regarding the definition of “gravitational energy” with respect to an arbitrary reference frame – given that, it remains a non-vanishing quantity in every frame of reference. This means, in particular, that the energy-momentum tensor in the presence of gravity remains to be a true tensor not only for linear space-time transformations, but – unlike the case for GTR – in all other admissible transformations between any two reference frames.

In YARK Theory, we arrive at the equivalence of gravitational and inertial masses similar to the widely acknowledged conceptualization of today – so much so, in fact, the proper mass of the test particle under gravity is cancelled out from the final equation of motion just like in GTR. As is well known, this property can be called the *weak equivalence principle*. Therefore, in YARK, particles with different rest masses do happen to acquire the same acceleration in a given gravitational environment. Moreover, the equivalence of gravitational and inertial masses always allows us to choose a reference frame whereby the local geometry becomes pseudo-Euclidean by intrinsic design.

Be that as it may, a particle in any such frame of reference undergoes to “experience”, so to speak, the presence of the gravitational medium simply due to the variance in its rest mass as compared to what it would have been in the absence of gravity.

Furthermore, in a synchronous reference frame attached to our test particle, which rests at the location defined by the position vector \mathbf{r}_m of the gravitational medium of concern, the space-time interval for *entire space* acquires the form

$$ds^2 = c^2 g_{00} dt_0^2 + g_{11} dx_0^2 + g_{22} dy_0^2 + g_{33} dz_0^2 = \left(1 - E_B(\mathbf{r}_m)/m_{0\infty} c^2\right)^2 (c^2 dt_0^2 - dl_0^2), \quad (3)$$

where $dl_0^2 = dx_0^2 + dy_0^2 + dz_0^2$.

Eq. (3) manifests a Minkowskian-like metric, where the Christoffel symbols for the *entire space* are equal to zero, and the diagonal metric coefficients $\{1, -1, -1, -1\}$ are multiplied by the factor $\left(1 - E_B(\mathbf{r}_m)/m_{0\infty} c^2\right)^2$; with the latter explicitly depending on the spatial coordinate of the particle of concern, and implicitly depending on time for a moving particle. Thus, in such a metric, the Christoffel symbols are equal to zero for *entire space-time*.

Defining the action for a test particle traversing a given path in such space as

$$S = -m_{0\infty} c \int ds, \quad (4)$$

and applying its variation in the metric (3), we get the Lagrangian

$$L = -m_{0\infty} e^{-\alpha(r_m)} c^2 \sqrt{1 - v_0^2/c^2}, \quad (5)$$

where $\alpha(r) = GM/rc^2$ in the radially-symmetric case. Here, G is the familiar gravitational constant, and M is the ponderable mass of our source of gravity.

In what follows, the energy of the gravitating test particle can be expressed as

$$E = \gamma m_{0\infty} e^{-\alpha} c^2. \quad (6)$$

It is easy to notice the similarity of Eq. (6) with the total relativistic energy obtained under the framework of GTR in the limit of a weak gravitational field:³³

$$m_\gamma c^2 = \gamma m_{0\infty} c^2 \sqrt{1 - 2\alpha} \approx \gamma m_{0\infty} c^2 (1 - \alpha), \quad (7)$$

which remarkably coincides with our total relativistic energy for a weak gravitational environment: $\gamma m_{0\infty} c^2 e^{-\alpha} \approx \gamma m_{0\infty} c^2 (1 - \alpha)$.

It would at any rate be fair to stress that, the first co-author had originally predicted all of these results without having to make use of the classical action principle and subsequent Lagrangian formalism – therefore relying on just the law of energy conservation embodying the mass and energy equivalence of STR [4,5].

In any event, both the YARK Equation (6) and GTR Equation (7) produce the same result up to the order of c^{-3} , and naturally both yield Newton’s equation of motion at the non-

relativistic limit. Therefore, YARK successfully provides explanations for cornerstone astrophysical observations in history (e.g., gravitational lensing, Shapiro delay, precession of the perihelion of Mercurial planets, gravitational redshift) otherwise considered as experimental confirmations of GTR.

Nevertheless, the strikingly overlapping outcomes of GTR's Eq. (7) and YARK's Eq. (6) to the calculation accuracy of c^{-3} does not mean that, both theories yield identical predictions all the way through even in the case of a weak gravitational field. For instance, mainstream cosmology has been challenged in ref. [25] to the effect that, a model of the Universe constructed according to YARK for a time epoch far removed from the presumed Big Bang event (where the approximation of the weak gravitational field then becomes applicable) specifically results in the elimination of the dark energy conundrum, brings about the alternating sign for accelerated cosmic expansion, leads to a derivation of the Hubble Constant, and helps account for other unusual observations in the Universe thus far unexplained by GTR [25].

It may also be mentioned in passing that, YARK successfully predicts and models "anomalous bending of gamma rays under Earth's gravity" as recently reported by V. Gharibyan from Deutsches-Elektronen Synchrotron (DESY).^{34,35}

One other principal aspect of YARK is the extension of Eq. (2) to any kind of force field when the binding energy E_B is properly framed in comparison with the case of gravity [14, 15, 18, 19]. For example, Eq. (2) remains valid for a test object with the proper mass m attached to the edge of a rotating disc [27]. In such a case, the static binding energy of the object is defined as the work that must be furnished to it in order to bring it quasi-statically from the rotational axis to the location with a radial coordinate r . Straightforward calculations yield $E_B = mu^2/2$, where u is the tangential velocity of the particle at the point r [27].

Using this definition of the static binding energy for a rotating system, and substituting the obtained value of E_B into Eqs. (2) and (3) through the framework of Yarman's Approach, we are able to offer a quantum mechanical explanation to a decades-long problem thus far unnoticed in modern spectroscopy; the puzzling presence of the extra-energy shift between emission and absorption lines in a rotating system, aside from the usual effect of relativistic time dilation owing to tangential displacement alone.³⁶

Concerning the expression for the relative energy shift between Mössbauer absorption lines $\Delta E/E = \pm ku^2/c^2$, the time dilation effect predicted by GTR is $k=1/2$ and *strictly nothing more*; whereas, according to our derivation based on YARK, it should come out to be $k=2/3$ for the Mössbauer rotor experiments under consideration – hence, in near perfect agreement with our latest findings of $k=0.66 \pm 0.03$,^{37,38} and $k=0.69 \pm 0.02$.³⁹

Eq. (2) moreover implies that, a neutral test object in the process of being flung across a centrifugal field should be jettisoning a minimal part of its rest mass as electromagnetic radiation [3, 36]. That is to say, the object of concern ought to irradiate (as seen by a co-rotating central observer) the rest mass deficit coming into play, all the while it gets hurled towards the rotor rim. Rephrased quantum mechanically (and in full conformance with YARK Theory) this entails a corresponding variation of discrete energy levels of constituent atoms of the test object. When such change in energy levels during varied acceleration of the object at hand engenders a corresponding increase of the static binding energy E_B , this should be accompanied by a commensurate electromagnetic emission as predicted by YA and substantiated in [3].

Concurrently, two principal predictions with respect to the properties of the anticipated electromagnetic radiation in the case of rotation have been made in [3]: i) The frequency of the radiation shall be governed by Eq. (1); ii) the spatial distribution of this radiation has to be essentially anisotropic and its intensity should draw a maximum toward the rotational axis. The reason for the latter is simple: The more attached an object becomes to the edge of the

rotating disc, the lesser its rest mass will turn out to be. Meanwhile, as binding intensifies in the centrifugal direction, discharge of radiation would escalate at the opposite direction (*i.e.* towards the center of rotation).

We want to add that, in an idealized case of stationary rotation (say, in empty space free of any friction), no radiation from electrically neutral bodies is expected. However, in a routinely encountered situation on Earth, where a “continuously powered” rotating object experiences incessant fluctuations in its angular acceleration due to unavoidable jabs of air friction delineated by the Maxwellian energy distribution, in addition to convection as well as hindrances caused by the axle, the outcome must differ. Radiation would be observed even when the average rotational frequency of the spinning item appears to remain constant to all intents and purposes.

Specific properties of the kind of radiation emanating from electrically neutral bodies allow us to identify it among other kinds of electromagnetic emissions. Our first experiment with the dental drill described in Sub-section 3.1 includes all pertinent features.

Radiation must, in fact, emerge from any type of non-constantly accelerating motion. Our second and third experiments described in Sub-sections 3.2 and 3.3 respectively provide additional support for emissions in such cases.

3. THREE EXPERIMENTS TO VERIFY ELECTROMAGNETIC RADIATION FROM VARIEDLY ACCELERATED NEUTRAL BODIES

We present hereunder the results of three separate experiments that each manifested the prediction made by Yarman’s Approach (YA). These experiments provide direct observational data of electromagnetic emissions at the expected frequency domain.

In our first experiment, we used a pneumatic dental drill to achieve a maximum angular velocity of about 400,000 rpm (*i.e.* 6500 rps on the average), where, in accordance with what had been established in ref. [3], radiation delineating an anisotropic spatial distribution in the ULF-VLF range up to 6.5 kHz was measured.

In a second experiment, colliding two empty gas cylinders of substantial mass against each other once more demonstrated the emergence of electromagnetic radiation within the expected range as a consequence of momentum gain surge from their impact surface areas.

In the third experiment, a set of steel strings under stereotypically high tension of a concert grand piano again yielded emanation in the anticipated frequency range when excited through forceful hammering by the keyboard mechanism; which is indicative of variegated acceleration, with respect time, of perturbed sections of the strings in like vein to the second experiment.

As shall be explained further down, the frequency of the registered electromagnetic radiation is attuned to the sound issued from the instrument used in all of the examples above. To put it in other terms, as long as sound production at the source is within the range of human hearing (*i.e.*, between 20 Hz – 20 kHz), plainly listening to the generated pitch offers a neat way of dynamically cross-checking the frequency of the emitted radiation.

One should note, however, that a trade-off takes place regarding the equipment’s sensitivity to detect emissions. Appertaining to our initial trial, the heavier the mass of the rotating object, the higher the amplitude of the emitted radiation; which would entail a better chance of frequency discernment. But on the other hand, it turns out to be much more difficult to accelerate a rotating body of great mass to high angular velocities – in which case, the frequency of the radiation (if any) would then be too low for detection.

In order to be able to detect electromagnetic radiation in the predicted ULF-VLF range of concern, we built a special loop antenna that was made using a copper wire 0.6 mm thick at a length of 100 meters wound about 40 times at an 80 cm radius. The loop antenna was then

connected to a complementary low-noise amplification circuit, onto which a low-noise integrated OP27G unit had been welded so as to achieve a clear signal boost.

After our preparation of the testing equipment was complete, we initialized SigView Spectrum Analyzer (®) software to check for incoming data through the MIC IN port of a PC laptop. Signals were successfully received from the already broadcasting VLF stations around our geographical location (Fig. 1).

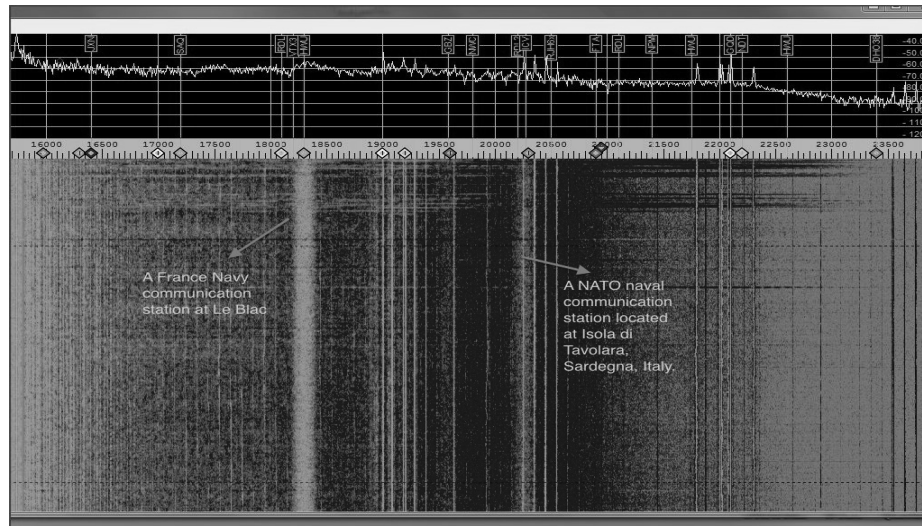


Fig. 1. Screenshot of SigView (®) software window, displaying the flow of registered VLF Station broadcasts that were being captured by our specially constructed loop antenna. A navy communications station at Le Blanc (France) transmits steadily at 18.3 kHz, and a NATO naval communication base located in Tavolara (Italy) transmits steadily at 20.27 kHz.

(Passage of time occurs in the vertical, against Hertz in the horizontal.)

Further swiveling or swooshing the loop antenna in any direction registered additional input, as would be expected from established electromagnetic theory as well as Yarman's Approach – albeit, with particular emphasis by the latter theory on radiation due only to varied acceleration, with respect time, in the case of electric charges – which, though, is outside the scope of this paper.

We then successfully tested the robust working of our antenna and related circuit through the utilization of a signal generator unit that was connected to an identically built transmitter antenna. Thus, when we transmitted at a given very-low or ultra-low frequency using the signal generator of concern, we were able to receive the broadcast straightforwardly by our primary antenna. In other words, any change in the frequency at the source was successfully relayed to and captured at the receiving end. Our team was therefore able to observe electromagnetic radiation above 100 Hz,* via employing just two antennae facing each other besides an ordinary amplification circuit to augment the signal intensity.

* It must all the same be stressed that, the metropolitan electricity infrastructure operating at constant 50-60 Hz presents a major source of contamination to the open testing environment, unless the equipment is specifically shielded against it. Nevertheless, instead of a recourse to expensive and cumbersome shielding, one can still confidently spot signals with equipment built from readily accessible materials, as long as the working frequency is chosen high enough above the infrastructure's, and that, a distinctive trail pattern is created at the source.

To gain more confidence about our enterprise, we repeated the same testing process with another program named Spectrum Lab (®), which, unlike its competitor, was further capable of demarcating signal strength in 2D via a color-coded spectrogram display.

Seeing more benefit in the indication of signal strength in 2D view, we decided to preliminarily continue forward using Spectrum Lab.

Either way, these programs were especially preferred for their reliance on the processing power of typical PC soundcards – facilitating, thereby, direct data feed from the easily accessible MIC IN port of a laptop computer.

Finally, it was possible to unmistakably discern electromagnetic emissions from the tools we used in our experiments as opposed to signal pollution from outside influences.

3.1. Radiation From a Pneumatic Dental Drill

We conducted a first set of experiments to measure radiation from a variedly accelerating neutral macroscopic body at a dental operating room reserved for the purpose. There, we were given leave to handle a modern pneumatic drill driven solely by an air compressor which resided outside the room, and which was powered down before each usage. Thus, we have good reason to believe no electromagnetic noise was introduced from the compressor during the entirety of running this setup; seeing as, it was filled in advance before each trial, and powered off during measurements. Strong contamination from the magnetic field generated by the compressor’s running motor would otherwise be noticeable on our evaluation screen – which we were then keen to summarily discard.

When our team held the drill’s bur toward the center of our stabilized loop antenna, and continuously varied its rotation via a control pedal between the whereabouts of 4500 rps and the specified maximum 6600 rps – as maintained in the official documentation⁴⁰ to denote the ultimate possible velocity the type of drill in question can attain – signal flow shown in Fig. 2 was registered.

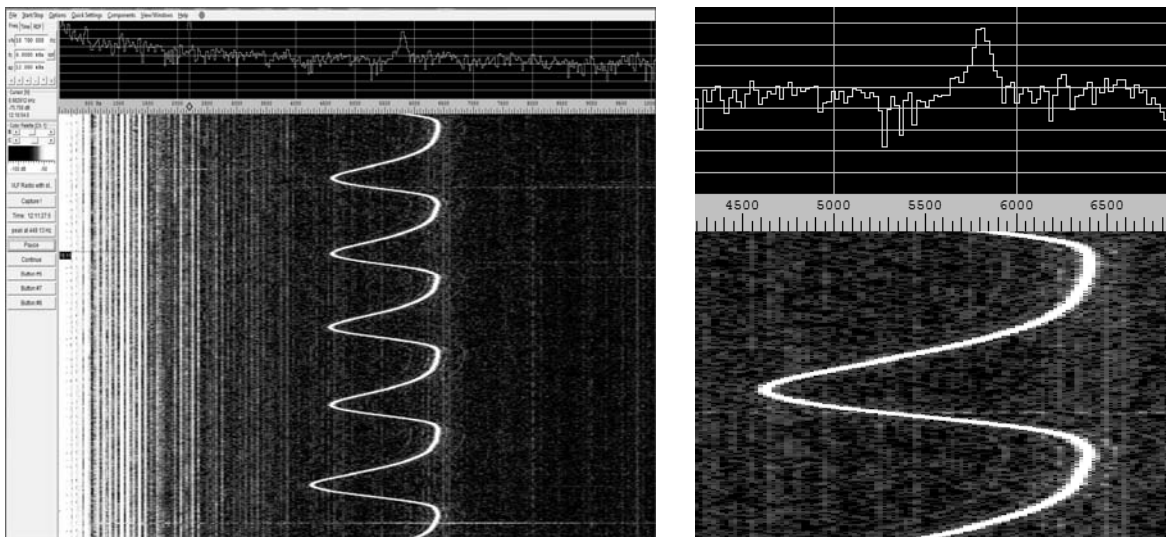


Fig. 2. Electromagnetic radiation being registered in Spectrum Lab (®). The unmistakable quasi-sinusoidal trail indicates emission history from the spinning bur of a pneumatic dental drill, as its angular velocity is periodically varied via a control pedal between the whereabouts of 200,000 RPM and the specified maximum 400,000 RPM. The frequency of the radiation is concurrently measured to oscillate between the 4.5 kHz and 6.5 kHz band. Signal continuum below 2.5 kHz is identified as persistent environmental background noise.

(Left: Screenshot of the Spectrum Lab software window, where passage of time in the vertical is against Hertz in the horizontal. Right: Zoom-in detail, where highest signal intensity is indicated by white, and possible harmonics are indicated by red arcs of weaker intensity.)

Signals detected below 2.5 kHz were identified as persistent environmental background noise owing chiefly to the electricity infrastructure. We base it on the fact that no significant change in this noise pattern was observed as long as the experiment was being performed. On the other hand, electromagnetic radiation in the frequency range predicted by Yarman's Approach was clearly distinguishable within the 4.5 – 6.5 kHz band, as seen in Fig. 2.

It should not escape the readers' notice that, the frequency of the emitted radiation is remarkably echoed as pitch of the same frequency – just like commonly heard as the familiar whizzing sound at the dentist's chair. Indeed, an average estimation of 6860 Hz by Altinoz et al.⁴¹ agrees with YA. Hence, plainly listening to the generated pitch can provide a neat way of dynamically cross-checking the prediction made by Yarman's Approach, so long as the sound is within the range of human hearing. The reason for this frequency concurrence shall be elucidated a bit further down in the text.

Understandably, we had no available means with which to quantify whether or not the spinning bur of the dental drill did in reality attain the maximum specified value. Nevertheless, it was clear to us that, unleashing the full power of compressed air would lead to the highest possible rotation very near factory specifications. One could, therefore, safely consign oneself to rely on the registered radiation frequency to estimate the exact angular velocity attained by the dental drill. In other words, for an ideal 6700 rps, Yarman's Approach anticipates electromagnetic radiation at 6700 Hz. Or the other way around, a radiation measurement of no more than 6500 Hz would entail that, the rotation is in fact 6500 rps instead of the prescribed peak value of 6700 rps. Indeed, we recorded emissions at a maximum frequency of 6500 Hz, which offers a strong validation for YA. This also means that the lower threshold of the frequency band under scrutiny was likely produced when the bur was spinning at around 4500 rps.

Even so, we need to analyze a plausible objection which can be raised against our findings.

Despite the above-given rationale and empirical evidence in favor of Yarman's Approach, it could yet be stated that, the dental bur becomes gradually ionized due to friction with air particles as it spins. This allegedly might be why we measure electromagnetic radiation throughout – *i.e.*, due to build-up of electric charges undergoing acceleration. As there seems to be no way of electrically grounding the bur component of the drill, such an objection would appear bothering at a first glance.

However, this counterargument against our experimental results is fundamentally flawed due to the following reasons:

Firstly, applying standard classical electrodynamics to the scenario at hand should cause a secondary effect which we haven't detected in any event. Since all accelerated charged particles that radiate must recoil as defined by the Abraham-Lorentz force, this would induce the increase of electrical potential in the bur in all radial directions on account of the centrifuge. But the force of reaction for radiation has the order of magnitude $(v/c)^3$, and the ratio $(v/c)^3$ at the tangential velocity $v=400$ m/s on the periphery of the drill (achieved at the highest 6600 rps rotation frequency for a bur with a radius of about 1 cm) indicates the order of 10^{-15} , which makes it wholly impractical to measure any effects related to the force of reaction for electromagnetic radiation.

Secondly, classical electrodynamics predicts isotropic radiation for ionizing atoms, but we recorded the strongest emissions at a specific direction with the spinning bur in conformance with Yarman's Approach – *i.e.*, from the lateral regions towards the axis of rotation perpendicular to the plane of the loop antenna (cf. ref. 3). And as it so happens, clearly weaker signals have been registered when the drill was held at a different angle to the loop antenna, as shown in Fig. 3.

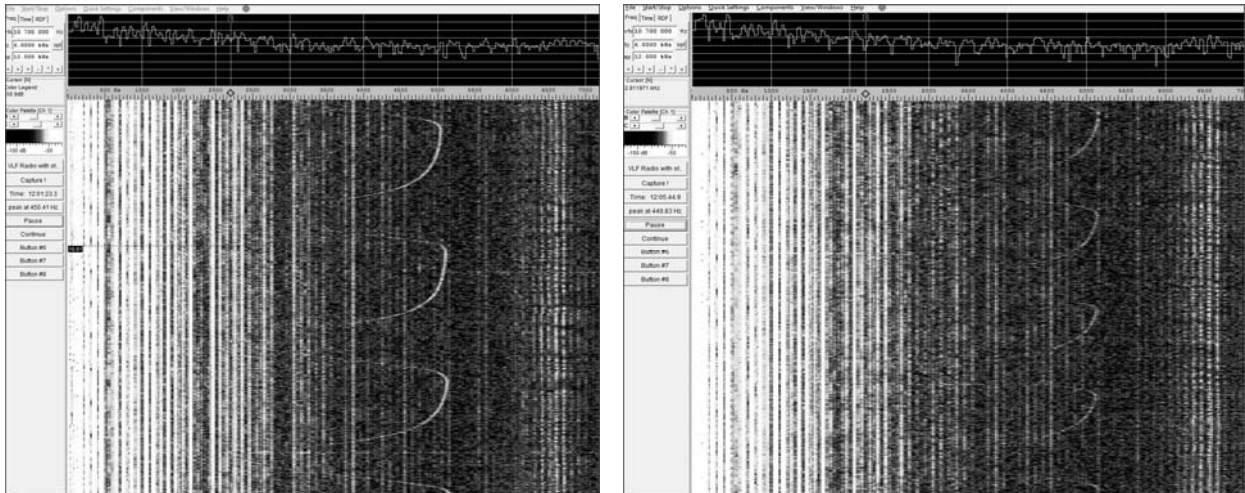


Fig. 3. Weaker electromagnetic radiation being registered in Spectrum Lab (®), due to holding the drill at a different angle to the loop antenna in conformance with Yarman’s Approach. The previously conspicuous quasi-sinusoidal trail, indicating emission history from the periodically varied spinning bur of a pneumatic dental drill, has now become much fainter. Radiation below 2.5 kHz is identified as persistent environmental background noise.

(Screenshots from the Spectrum Lab software window, where passage of time in the vertical is against Hertz in the horizontal.)

Thirdly, a distinguishing feature of Yarman’s Approach is laid bare further down in Fig. 4. According to our theoretical model, the emission slope of the increasing acceleration rate will be gentler than the slope of the decreasing rate of deceleration. This is due to the inertia of the former being more pronounced than the inertia of the latter; because the force of friction acts more strongly when the bur jump-starts compared to when it is in a state of motion. As a consequence, we predict intensification of irradiation as the bur gradually gets more and more freed from the drag of friction in higher rotational velocities, so long as continuous power supply is maintained.

Additionally, Yarman’s Approach states that, radiation shall still keep on being emitted during “stabilized rotational speed”, and even after the power is cut off, on account of tangential stuttering and rebound of the bur as it interruptedly brakes with non-uniformly acting air friction delineated by the Maxwellian energy distribution (if we may overlook the hindrances caused by the axle). No further radiation is expected otherwise in vacuum conditions; except possibly due to material irregularities in the bur manifesting as resistance against stationary rotation.

Let us note that, the sudden jolt of acceleration when the power supply is restored once more will cause momentary intensification of electromagnetic emissions for causes just now explained, and as seen in Fig. 4.

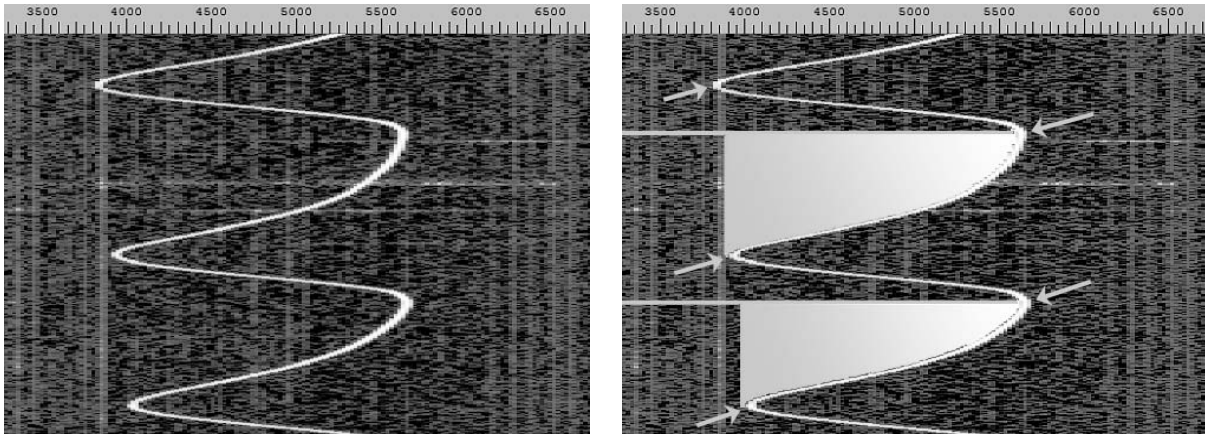


Fig. 4. Electromagnetic radiation being registered in Spectrum Lab (®). The quasi-sinusoidal trail between the 3.8 kHz and 5.7 kHz band (coinciding with repeated manual firing and release of the drill between more or less 230,000 RPM and 340,000 RPM angular velocities respectively) exhibits a peculiarity unique to Yarman’s Approach. The ascending slope designates emission from the bur during the increase in the rate of acceleration, which is markedly gentler than the descending slope, indicative of emission during decrease in the rate of deceleration, following the cut-off of power. Turning points delineated by arrows denote maximal intensification of radiation due to explained effects of air friction.

(Left: Snapshot from the Spectrum Lab software window, where passage of time in the vertical is against Hertz in the horizontal. Right: Detailed inspection, where highest signal strength is indicated by white, and moments of greatest intensification demarcated by arrows.)

Fourthly, attributing the observed radiation to ionization of either the metallic bur of the drill or surrounding air particles is extremely unrealistic, simply because emissions have been registered at the range of very low frequencies. This means that, metallic ionization is not in the least possible at such energy levels, and that, even air-bound ions can under no circumstances keep on spinning with the bur without getting kicked out by the centrifugal force for even a few revolutions, let alone thousands of times per second, to be the cause of the detected emissions.

On top of these, non-uniformly acting air friction – *as the reason behind the previously explained tangential stuttering and rebound of the bur during a seemingly constant (i.e., imperceptibly and unpreventably wavering) angular velocity* – leads to the commonly heard shrill sound alongside the frequency of the emitted radiation. It is, as we can tell, the result of minute acoustic perturbations in the surrounding atmosphere each time the power supply compensates for the fallback of the bur to a lower rotational speed due to ever-present and naturally fluctuating air friction (as described in ref. 3).

Let us elucidate this important feature in greater detail: The dental drill rotates at any instantaneously given quantum mechanical state according to Yarman’s Approach [3] – even when the quantization of the energy levels of concern turns out to be inconspicuous in everyday macroscopic experiments. If there were no air particles scraping on the bur component, it would keep on spinning indefinitely without a power supply; provided that, we forgo any hindrances caused by the axle as previously argued. But once the experiment at hand is conducted in an open environment, the drill naturally faces instabilities (no matter how minute) due to friction, as well as in the power supply. Now, what would make the bur emit radiation a final time before it reaches its true stationary velocity under vacuum conditions? That would indeed be its last quantum mechanical micro-jump in getting further bound to its terminal stationary state via a final modicum of increase in the intensity of the centrifugal force.

But once the experiment of concern is conducted in an open environment, the drill naturally faces instabilities in air friction as well as in the power supply. As a result, whenever the torque induced by friction is just a bit greater than the torque which assures constant rotation, the bur would immediately recede to a lower quantum mechanical rotational level [3] – and whenever the torque overcomes air friction owing to the uninterrupted power supply, the bur would climb back up to a higher quantum level. So, each time the bur drops to a lower rotational velocity, it is on account of a non-uniform friction; and each time the bur is brought back up, it is due to the compensation by the uninterrupted power supply.[†]

Hence, every instance of restoring the bur to its higher quantum mechanical state of rotation is expected to produce electromagnetic radiation at frequencies dictated by Eq. (1) – whereas, the heard sound frequency is conversely generated at every instance the bur imperceptibly slows down with friction, which simultaneously leads to the perturbation of the atmosphere in the immediate vicinity. In other words, when neighboring gas molecules lend an exiguously greater-than-nominal portion of their energy to the rotating drill, and the bur thus piles up a commensurate amount of rest mass that causes it to momentarily decelerate, adjacently disturbed air particles gain an analogous vitality for propagating acoustic vibrations.

This recurrent process throughout a seemingly stationary (*i.e.*, infinitesimally wavering) angular velocity betokens the consecutiveness of, or interplay between, the mentioned two phenomena at the same frequency for low atmospheric pressures – which is our ratiocination of howcome the two kinds of frequencies effectively coincide.

All these subtleties render Yarman’s Approach singularly distinct, as compared to standard classical electrodynamics, in terms of explaining the detected electromagnetic radiation from a pneumatic dental drill.

3.2. Radiation From Striking Two Empty Gas Cylinders Against Each Other

In our second trial, we collided two empty gas cylinders of substantial mass against one another, while the receiving antenna was suspended sideways nearby inside a Faraday Cage. Signal intensity depended on the forcefulness of the crash – therefore, it took some effort to lean the cylinders against each other by two members of our team, while a third participant stabilized the loop antenna beside them; to the extent that, the antenna’s center was precisely next to their impact points.

At this juncture, we reverted to using SigView (®) to analyze the incoming signals for the benefit of its 3D spectogram display.

Prior to conducting this trial, we ascertained that the SigView software recorded purity when the loop antenna was hanging inside the Faraday Cage, as seen in the output of Fig. 5.

In contrast to the foregoing signal purity, moments of impact revealed noticeable electromagnetic disturbance as presented in Fig. 6.

Although the basic physics behind this experiment is similar to the one with the non-constantly accelerating disc (*e.g.*, the spinning bur of the dental drill explained under Subsection 3.1), an exact model of the varied momentum gain of constituent atoms at the moment of impact is time-consuming to fashion, and hence, requires separate attention. All the same, we can establish from Eq. (1) that, the frequency of the registered electromagnetic radiation must accompany a similar sound frequency reverberating in the air.

[†] In just the same way, sustained periodical oscillation of a diminutive magnitude should transpire in all “non-ideal” stationary velocity scenarios.

That being the case, the second co-author is able to attest to such a fact as a musician with an absolute ear faculty; to the effect that, the heard tone is perceived to be near the Western Concert Pitch A4.

Of course, future experiments on the synchronous measurement of both the radiation and the issued sound would provide higher accuracy for Yarman's Approach.

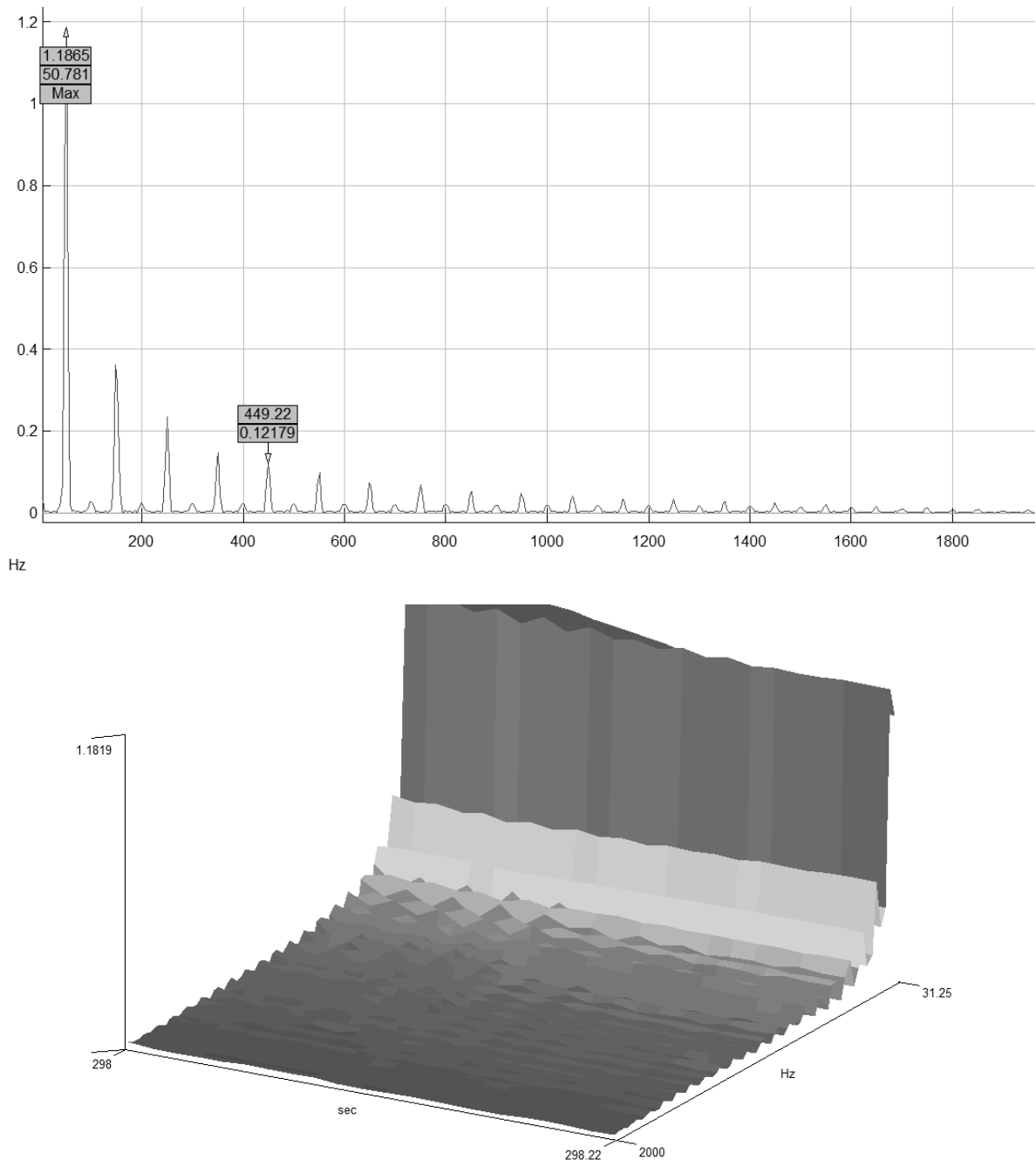


Fig. 5. Electromagnetic purity being registered in SigView (®), on account of the loop antenna being suspended inside a Faraday Cage.

(Above: 2D view, where intensity in the vertical is against Hertz in the horizontal. Below: 3D view, where x-axis indicates time, z-axis indicates frequency, and y-axis indicates magnitude of the signal.)

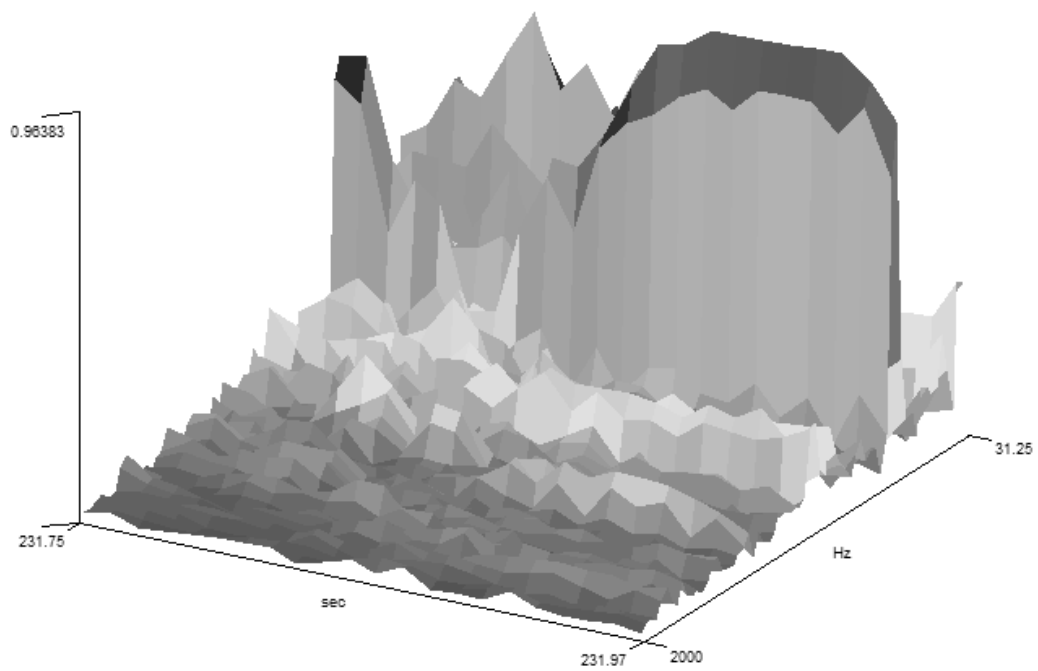
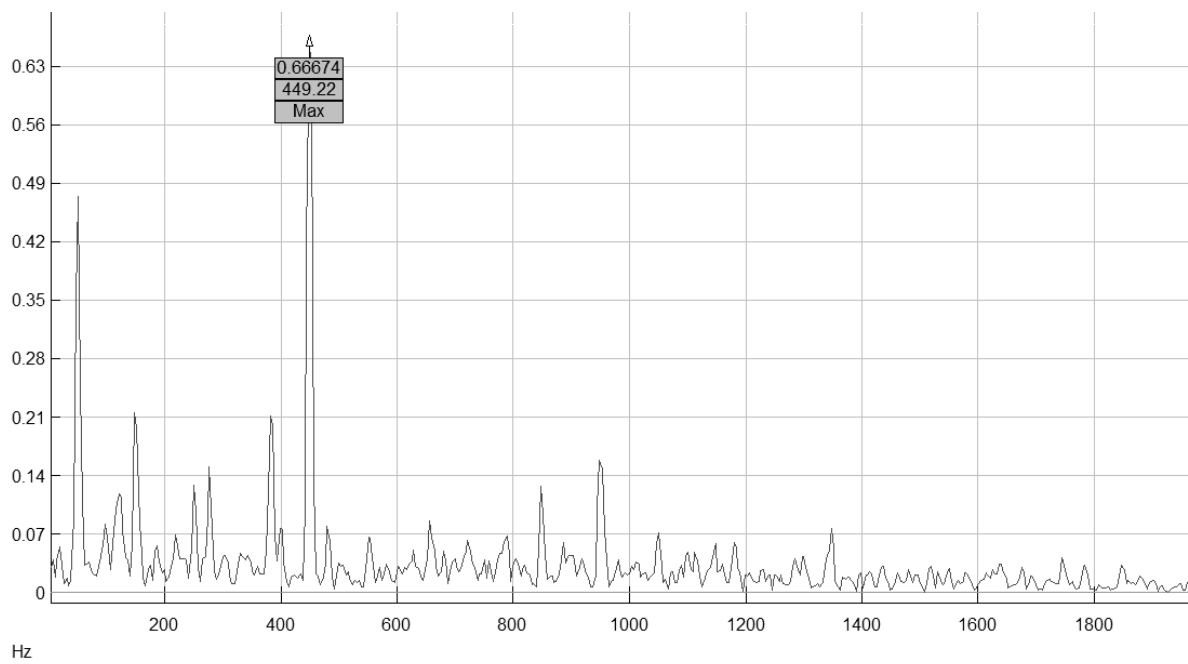


Fig. 6. Salient electromagnetic disturbance being registered in SigView (®) subsequent to the head-on collision of two empty gas cylinders.

(Above: 2D view, where intensity in the vertical is against Hertz in the horizontal. Below: 3D view, where x-axis indicates time, z-axis indicates frequency, and y-axis indicates magnitude of the signal.)

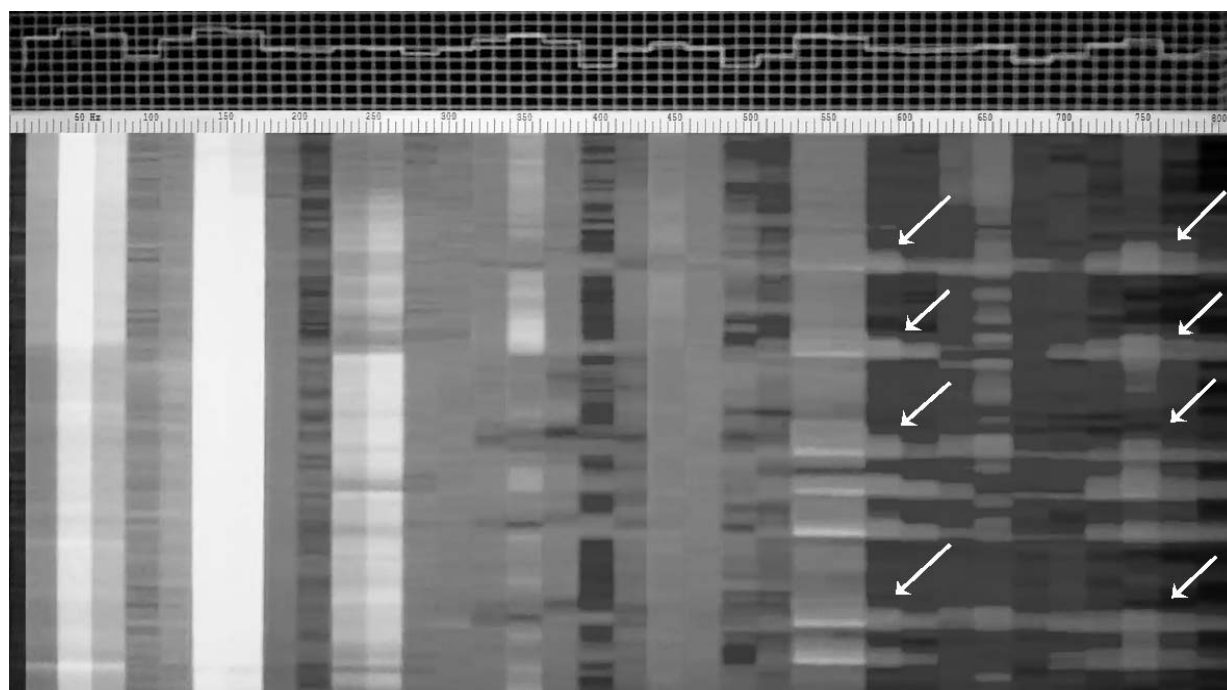
3.3. Radiation From a Concert Grand Piano

Having previously experienced certain difficulties at testing Yarman et al.'s hypothesis in several precursory attempts with rotating appliances, the second co-author suggested, at the outset, that we focus on a purely mechanical, percussive approach, where electromagnetic radiation from acoustic vibrations could be measured instead. In what would later inspire our second experiment with crashing cylinders, the second co-author came up with the idea of placing the loop antenna horizontally on top of the iron frame of his Bechstein B204 model concert grand piano while he played on the keyboard.

The instrument in question – tuned to a near equal temperament[‡] at A4=440 Hz pitch level – incorporates 226 rigid steel (for middle to treble registers) and copper-wound steel (for bass registers) wires (corresponding to 88-keys; of which 52 are white, and the remaining 36, black) under stereotypically high tension, altogether said to exceed 20 tonnes of tensile force.⁴²

What followed next was the placement of the loop antenna flatly on the inside of the concert piano: That is to say, at a resting position over the iron frame.

When the second co-author executed wide chromatic tone-clusters in an idiosyncratically syncopated and fortissimo fashion – exciting simultaneously, therefore, a broad array of piano strings via repeated hammer strikes – the distinctive radiation spread shown in Fig. 7 was registered on our monitor.



[‡] To be more precise, “Ultimate Synchronous Beating Well-Temperament 4b” devised by Ozan Yarman (accessible from the SCALA Scale Archive by Manuel op de Coul and Aaron Andrew Hunt: <http://www.h-pi.com/scalavista>), which gives rise to vibrant key colors on different tonalities, that are otherwise unavailable with the standard Equal Temperament of Western music.

Rhythmic Tone Clusters for an Experiment to verify Yarman's Approach

Ozan Yarman

Copyright © 2013-2015

Fig. 7. Electromagnetic radiation being registered in Spectrum Lab (®). Interruptive streaks from 500 Hz to 800 Hz coincide with characteristically syncopated tone-clusters at fortissimo dynamics on an acoustic grand piano. Execution on the keyboard triggers hammer strikes on the related 150 or so strings, which results in variegated acceleration of perturbed sections of said strings – causing, therefore, emissions in conformance with the prediction made by Yarman’s Approach. Persistent radiation in the vicinity is identified as environmental background noise.

(Above: Snapshot from the Spectrum Lab software window, where passage of time in the vertical is against Hertz in the horizontal, with arrows acting as guides to temporal locations of notated tone-clusters. Below: Musical notation of the played tone-clusters, with arrows acting as guides to temporal locations of recorded streaks.)

Here again, the basic physics is analogous to the non-constantly accelerating dental bur, and poses the same problem as the second experiment involving two collided cylinders: It is laborious to fashion a satisfactorily precise model of the varied momentum gain of the alloy constituents of excited steel strings.

Nonetheless, just like it had been elaborated previously with regards to the dental drill, we expect the frequency spectrum of the recorded electromagnetic radiation to accord with the pitch of the 49 clustered notes on the piano from C2 to C6. As it so happens, one can clearly see that this is more or less the case with Fig. 7.

On account of this fine match, and having a pressing concern about already overloading the present article, we postpone relevant calculations on the direct derivation of the expected radiation frequencies to a subsequent paper.

To be completely sure that it was not the shaking of the iron frame, nor uplifted air, that disturbed the antenna to cause any unwanted parasite signals, we later fixed the loop antenna a little above the strings with no part of it contacting the piano frame or case. The result was observed to be thoroughly the same.

Note anyway that, the radiation is abruptly cut off upon the player’s release of the keys, since the strings do not keep on resonating after the dampers of the keyboard mechanism come down.

It goes without saying that, a change in sound amplitude does not cause the frequency to vary for any given string or course of strings.

At the end of the day, rhythmically varied tone-cluster keyboard playing by the second co-author, which caused massive and forcible excitation of about 150 piano wires, confirmed most conclusively that, electromagnetic radiation occurs at the frequency range predicted by Yarman’s Approach.

We have thus incontrovertibly observed the following milestones in our experiment with the piano:

- o The frequency spectrum anticipated by YA was reflected back at the screen of Spectrum Lab software, which had been connected to our receiver antenna via the previously mentioned portable setup.
- o Observed frequency distributions and patterns were coincident with forcibly coming down with both arms on the keyboard across note C2 (65.5 Hz) to note C6 (1049 Hz) in a syncopated manner.
- o Extraction of notes from the tone-cluster, or just playing simple chords, diminished the chances of seeing changes on the screen.

4. DISCUSSIONS AND CONCLUSION

A series of experiments conducted by our team have manifested the prediction made by Yarman's Approach (YA) [3], where neutral bodies are posited to emit electromagnetic radiation due only to changes in the rate of acceleration. According to YA, neutral bodies should thus exhibit emissions in both rotational and translational non-constant acceleration scenarios.

We anticipate radiation to follow a quantitatively small loss of rest mass on account of the object getting bound to its accelerational field, which is a requirement of the law of energy conservation embodying the mass-energy equivalence of the Special Theory of Relativity (STR) under the framework of YA.

This process can be better comprehended as follows: When paired or conglomerated particles (*e.g.*, protons and electrons making up an atom) interact more intensely with each other, they move just a little bit away from one another as compared to before – regardless of the gravitational, electric or centrifugal field involved. Hence, in the case of atoms that bind more strongly, the distance between electrons and nucleons ought to *stretch* as much as the binding energy difference coming into play. This framework has been thoroughly explained in references [3,11,12].

A distinctive feature of the electromagnetic radiation predicted by Yarman's Approach [3] is its universally anticipated emergence from both neutral and charged non-constantly accelerating bodies. Thus, the intensity of the emitted radiation should depend on just the change in the rate of acceleration; which is unlike classical electrodynamics (CED), where constantly accelerated charges are also said to radiate. The non-trivial nature of this assertion, as well as having exhausted article space, prevents us from delving into particulars.

The extended YARK (Yarman-Arik-Kholmetskii) Theory can moreover be applied to answer for radiation from accelerating charges in cyclotrons [3,11,12]. While such an endeavor is best left to a subsequent article, the present cast, as discussed in ref. [3], already accords with the Larmor prediction for power emitted by such an accelerating particle.⁴³

To test the hypothesis of YA regarding electromagnetic radiation from variedly accelerating neutral macroscopic entities, our team carried out three separate trials.

In our first and most recent experiment, we held close to a specially constructed loop antenna a pneumatic dental drill that was said to climb up to about 400,000 rpm, and was driven solely by a powered-down air compressor (eliminating, thereby, any risk of electrical interference); which clearly manifested the reception of electromagnetic radiation (delineating an anisotropic spatial distribution) in the ULF-VLF range up to 6.5 kHz. Recorded signals were thence observed to be in exceptional harmony with Yarman's Approach.

Two key findings with regard to the first experiment were the following: i) For a circular motion with associated variance in angular acceleration, the modulus of the radiation

frequency was identical to instantaneous revolutions per second. ii) The spatial distribution of radiation intensity is highly anisotropic, as had been predicted by Yarman’s Approach [3].

It should also be emphasized that, in all of the performed experiments, the frequency of the electromagnetic radiation turned out to be the same as the sound frequency that had been issued to the surrounding air. Such is clearly the case for the typically shrill sound of the dental drill coinciding with emission frequencies from the variedly accelerated spinning bur.

Next, we elaborated on an earlier experiment which involved the head-on collision of two empty gas cylinders against one another, that revealed radiation ensuing from neutral bodies once again. Recorded signals from this second experiment matched the predictions of YA with regard to the radiation frequency equalling the issued sound frequency.

In a third experiment, a set of steel strings under stereotypically high tension of a grand piano again irradiated in the expected frequency range when excited through forceful hammering by the keyboard mechanism, which was indicative of variegated acceleration of perturbed sections of the strings. Just as before, captured signals were demonstrative of the correlation of electromagnetic emission frequencies with produced sound frequencies, confirming the forecast of Yarman’s Approach anew.

The third experiment reveals a noticeable benefit for the music industry: By utilizing a more sensitive and target-specific loop antenna, and then simply recording electromagnetic emissions from a Faraday-shielded acoustic instrument such as the piano, it could be possible to transcribe live polyphonic notation of the music played, without having any need for unrewardingly cumbersome pitch analysis techniques such as Fast Fourier Transform.

Our hitherto empirically substantiated theoretical model can further shed light on the so far inadequately explained *sonoluminescence* – *i.e.*, emission of visible light when a gas bubble formed via ultrasonic waves at the center of a flask of fluid is further compressed.⁴⁴

Let us evaluate this phenomenon more closely from the perspective of YARK Theory.

At the first stage, externally introduced ultrasonic energy begins to concentrate at the center of the flask, and transforms water molecules there into vapor – thus creating a “gas bubble” inside the fluid. Notwithstanding, this bubble continues to receive further sonic energy, and, as a result, gets more and more heated up – eventually reaching thousands of degrees Kelvin. During this time, the bubble gradually expands; or in other words, its gas constituents keep gaining so much kinetic energy that they start to push away the surrounding liquid via a transfer of energy and momentum. Sooner or later, the enveloping liquid constituents run out of space to retreat, since liquid atoms and molecules are electrostatically repelled by their neighbors. Meanwhile, the barricaded atoms and molecules of the liquid continue to compile surplus energy as extra rest mass (or *rest energy*, were speed of light taken unity) at a given “metastatic level” (similar to a maximally squeezed spring). Following the steady reception of additional energy, the bubble reaches a critical point whereby it can no longer sustain its expanded volume, and finally implodes.

At this second stage, the bubble undergoes a cataclysmic collapse. Extra rest mass is progressively discharged as electromagnetic radiation all the way up to visible light during the enveloping liquid’s rush to the center of the bubble from all directions. As a consequence of this, radiation is emitted omni-directionally as predicted by YA.

At the third stage, following sonoluminescence, the bubble bounces in size a few times until it stabilizes, and then repeats the same process, as long as acoustic energy is kept on being delivered to the medium.

YARK Theory is able to come up with a derivation for the sustained power P of the sonoluminescing bubble as [3]:

$$P = m \left| \frac{da}{dt} \right| R \quad , \quad (8)$$

where m is the mass of the bubble, da/dt , the rate of change in the acceleration of the collapse, and R the radius of the bubble.

P , R , and da/dt are normally functions of time; but the sustained power P in the case of sonoluminescence is evidently proportional to the sonic power \mathcal{P} delivered by the loudspeakers to the fluid flask. All of these quantities can be visualized at their averaged values prior to the emission of radiation. In the equation above, the average radius R of the collapsing bubble can further be associated with the wavelength λ of the emitted light – while, on the other hand, one can propose to write the time dependency of the bubble radius as $r(t) \sim t^3$ for derivational convenience geared to assess da/dt .

We can ultimately express the sustained sonoluminescence power P of the radiation – or relatedly, the sonic power \mathcal{P} – in terms of the intracavity average density $\bar{\rho}$ of the compressed air bubble, wavelength λ of the observed radiation, and duration τ of the implosion time period; hence as

$$\mathcal{P} \sim \rho \lambda^5 / \tau^3, \quad (9)$$

which happens to be in striking agreement with the available data on this topic.[§]

We particularly wish to underline YARK Theory's vital prediction that, the entire electromagnetic spectrum from the lower regions up until the emergence of visible light ought to be swept during the collapse event of the bubble, and this would be associated with successive quantum increases governed by the da/dt parameter in Eq. (8). Therefore, we anticipate frequencies lower than observed light to precede the radiation in the visible spectrum – especially in the infrared, and possibly in the microwave regions – after bubble collapse starts. That being the case, electromagnetic radiation of lesser frequencies should be expected just before sonoluminescence, and straightforwardly measured through proper equipment. Detailed analysis, however, must be considered elsewhere.

Lastly, focusing on the ~1 Hz to 20 Hz seismic noises that originate from the Earth's crust, and comparing these infrasound patterns with electromagnetic emissions theorized by YA to emanate from tectonic plates pressing against one another, can constitute a powerful preemptive method for detecting earthquakes before they strike. We can confidently assume that, fault lines on the verge of being fractured will register an alarming rise in the intensity of electromagnetic radiation compared to tranquil times.

ACKNOWLEDGEMENTS

We owe many thanks to the Faculty Members of Marmara University (MU) Faculty of Dentistry, and also to the Faculty Members of the High-Energy Laboratory under the Faculty of Electric and Electronics Department of Istanbul Technical University (ITU), for providing us with the opportunity to realize our first and second experiments. Special thanks thus go to Prof. Mahir Günday, Prof. Dr. Hesna Sazak Öveçoğlu, Prof. Yildiz Garip Berker, Assist. Prof. Sertaç Peker from MU, and Prof. Özcan Kalenderli, as well as to Prof. Kevork Mardikyan from ITU, in appreciation of their prestigious efforts that lead to the verification of our theoretical work. We further convey our appreciations to Dt. Natik Ergün, Dt. Fatih Bilen, and Dt. Özgür Aydemir, for their exceptional hospitality in helping us to conduct our drill

[§] Taking the bubble intracavity temperature as 20,000 Kelvin degrees, and gas pressure as 3,000 Bars gives us 0.05 kg/m^3 gas density. Implosion time is considered as 100 picoseconds, and wavelength of visible light is inputted as $\lambda \approx 5 \times 10^{-7} \text{ m}$. The result is around 40 Watts power output, which is quite reasonable when we consider the power output of the ultrasonic speakers used in sonoluminescence experiments.

experiment at their professional facilities. Lastly, we are grateful to Dr. Fatih Özyaydin and Dr. Ali A. Altintas in supporting and evaluating our work.

REFERENCES

- ¹ L. L. DeRaad Jr, T. Erber, Appl. Phys. Lett., **33**, p. 908 (1978).
- ² A. Belyanin, V. Kocharovsky, V. Kocharovsky, F. Capasso, Phys. Rev. Lett., **88**, 053602 (2002).
- ³ T. Yarman, M. Arik, A. L. Kholmetskii, Eur. Phys. J. Plus, (2013).
DOI: 10.1140/epjp/i2013-13134-9.
- ⁴ T. Yarman, Annales de la Fondation Louis de Broglie, **29**, Issue 3 (2004).
- ⁵ T. Yarman, Foundation of Physics Letters, **19** (2006).
- ⁶ T. Yarman, Int. J. Phys. Sci. **5**, p. 2679 (2010).
- ⁷ T. Yarman, Int. J. Phys. Sci. **6**, p. 2117 (2011).
- ⁸ T. Yarman, *The Quantum Mechanical Framework Behind the End Results of the General Theory of Relativity: Matter Is Built on a Matter Architecture*, Nova Publishers, New York (2010).
- ⁹ T. Yarman, Chimica Acta Turcica, **26**, Issue 3 (1998).
- ¹⁰ T. Yarman, International Journal of Theoretical Physics, **48**, Issue 8, p. 2235 (2009).
- ¹¹ T. Yarman, Scaling Properties of Quantum Mechanical Equations, Working As The Framework of Relativity: Principal Articulations About The Lorentz Invariance Structure of Matter, Physics Essays, **26**, Issue 4, pp. 473-494 (2013).
- ¹² T. Yarman, Scaling Properties of Quantum Mechanical Equations, Working As The Framework of Relativity: Applications Drawn by a Unique Architecture, Matter Is Made of, Phys. Essays, **27**, Issue 1 (2014).
- ¹³ T. Yarman, *Physical Interpretation of Relativity Theory: Proceedings*, Moscow, 4 - 7 July 2005 / Edited by M.C. Duffy, V.O. Gladyshev, A.N. Morozov, P. Rowlands - Moscow: BMSTU PH (2005).
- ¹⁴ T. Yarman, A Novel Approach to the End Results of the General Theory of Relativity and to Bound Muon Decay Rate Retardation, *DAMOP Meeting*, APS, 16-19 May 2001, London, Ontario, Canada.
- ¹⁵ T. Yarman, A Novel Approach to the Bound Muon Decay Rate retardation: Metric Change Nearby the Nucleus, *Physical Interpretation of Relativity Theory: Proceedings*, Moscow, 4-7 July 2005 / Edited by M.C. Duffy, V.O. Gladyshev, A.N. Morozov, P. Rowlands - Moscow: BMSTU PH (2005).
- ¹⁶ T. Yarman, Superluminal Interaction Making the Basis of Quantum Mechanics, Academic Publication, Lambert (2011).
- ¹⁷ T. Yarman, A. L. Kholmetskii, M. Arik, arXiv:1401.3110
(<http://arxiv.org/ftp/arxiv/papers/1401/1401.3110.pdf>).
- ¹⁸ T. Yarman, Vladislav B. Rozanov, The Mass Deficiency Correction to Classical and Quantum Mechanical Descriptions: Alike Metric Change and Quantization Nearby an Electric Charge, and a Celestial Body - Part I: A New General Equation of Motion for Gravitationally or Electrically Bound Particles, International Journal of Computing Anticipatory Systems, Partial Proceedings of the Seventh International Conference CASYS'05 on Computing Anticipatory Systems, Liège, Belgium, August 8-13, 2005, D. M. Dubois (Ed.), Published by CHAOS, **17** (2006), pp. 172-200 (ISSN 1373-5411, ISBN 2-930396-03-2).
- ¹⁹ T. Yarman, Vladislav B. Rozanov, The Mass Deficiency Correction to Classical and Quantum Mechanical Descriptions: Alike Metric Change and Quantization Nearby an

-
- Electric Charge, and a Celestial Body - Part II: "Quantum Mechanical Deployment for Both Gravitationally and Electrically Bound Particles", International Journal of Computing Anticipatory Systems, Partial Proceedings of the Seventh International Conference CASYS'05 on Computing Anticipatory Systems, Liège, Belgium, August 8-13, 2005, D. M. Dubois (Ed.), Published by CHAOS, **17** (2006), pp. 172-200 (ISSN 1373-5411, ISBN 2-930396-03-2).
- 20 T. Yarman, M. Arik, A. L. Kholmetskii, Turkic World Mathematical Society (TW MS), Journal of Applied Engineering and Mathematics, **1**, Issue 1, pp. 109-125 (2011).
- 21 T. Yarman, M. Arik, A.L. Kholmetskii, A Critical Analysis of Einstein's Non-Conform Analogy Between Rotation and Gravitation - Part II: Harmony Between Non-Locality and STR in Both Micro and Macro Worlds, in Mathematics, Physics and Philosophy in the Interpretations of Relativity Theory II, 4--6 September 2009, Budapest available at http://www.phil-inst.hu/~szekely/pirt_bp_2/papers/papers.htm.
- 22 T. Yarman, A. L. Kholmetskii, Ö. Korfali, International Journal of the Physical Sciences, **5**, Issue 10, pp. 1524–1529, 4 September, 2010.
- 23 T. Yarman, A. L. Kholmetskii, M. Arik, International Journal of the Physical Sciences, **6**, Issue 19, p. 4571, 16 September (2011).
- 24 T. Yarman and A. L. Kholmetskii, *Chinese Physics, B*, **20**, 105101 (2011).
- 25 T. Yarman, A. L. Kholmetskii, Sketch of a Cosmological Model Based on the Law of Energy Conservation, *Eur. Phys. J. Plus*, **128**, Issue 8 (2013).
- 26 G. Sobczyk, T. Yarman, Applied and Computational Mathematics, An International Journal, December 2008.
- 27 T. Yarman T, V. B. Rozanov, M. Arik, 2007 Proc. Int. Meeting on Physical Interpretation of Reality Theory (Moscow, 2-5 July 2007) ed M C Duffy et al (Moscow: BMSTU PH),
- 28 T. Yarman, M. Arik, A. Kholmetskii, A. A. Altintas, F. Ozaydin, Alpha Head on Collision with a Fixed Gold Nucleus, Taking into Account the Relativistic Rest Mass Variation as Implied by Mass - Energy Equivalence, *Acta Physica Polonica A*, **125**, Issue 2, p. 609 (2014). DOI: 10.12693/APhysPolA.125.609.
- 29 T. Yarman, A. L. Kholmetskii, Just Like The Gravitational Field, The Electric Field Too, Slows Down A Clock, Interacting with it: A Whole New Approach To The Bound Muon Decay Retardation, *Physical Interpretations of Relativity Theory*, 12-15 September 2008, London.
- 30 T. Yarman, A. L. Kholmetskii and O. V. Missevitch, *International Journal of Theoretical Physics*, **50**, Issue 5, pp. 1407-1416 (2011).
- 31 T. Yarman, M. Arik, A. L. Kholmetskii, A Prediction Regarding the Weakening of the Blue Shift of Light From Geosynchronous Satellites, Turkic World Mathematical Society (TW MS), *Journal of Applied Engineering and Mathematics*, **1**, Issue 1, 2011, pp. 109-125.
- 32 T. Yarman, A. L. Kholmetskii, M. Arik, O. Yarman, Novel Theory Leads To The Classical Outcome For The Precession of The Perihelion of a Planet Due To Gravity, *Physics Essays*, **27**: pp. 558-569 (2014).
- 33 L. D. Landau, E. M. Lifshitz, *The Classical Theory of Fields*, Chapter 10, Paragraph 88, (Butterworth & Heinemann, 1999).
- 34 <http://arxiv.org/pdf/1401.3720.pdf>
- 35 M. Arik, T. Yarman, A. L. Kholmetskii, O. Yarman, "Yarman's Approach Predicts Anomalous Gravitational Bending Of High-Energy Gamma-Quanta", Article Recently Accepted for Publication in *Canadian Journal of Physics* (Manuscript cjp-2015-0291).

-
- ³⁶ T. Yarman, A.L. Kholmetskii, M. Arik, Mössbauer Experiments In A Rotating System: Recent Errors And Novel Interpretation, Paper Under Review in EPJ Plus.
- ³⁷ A. L. Kholmetskii, T. Yarman, O. V. Missevitch, B. I. Rogozev, A Mössbauer Experiment in a Rotating System on the Second-Order Doppler Shift: Confirmation of the Corrected Result by Kündig, *Physica Scripta*, **79**, Issue 6, 2009.
- ³⁸ A. L. Kholmetskii, T. Yarman, O. V. Missevitch, Mössbauer Experiment in a Rotating System: The Change of Time Rate For Resonant Nuclei Due To The Motion And Interaction Energy, *Il Nuovo Cemento B*, **124**, Issue 8, pp. 791-803, 2009.
- ³⁹ T. Yarman, A. L. Kholmetskii, M. Arik, B. Akkus, Y. Oktem, L. A. Susam, O. V. Missevitch, Novel Mössbauer Experiment in a Rotating System and The Extra-Energy Shift Between Emission and Absorption Lines, Article accepted for Publication by the Canadian Journal of Physics (Manuscript cjp-2015-0063).
- ⁴⁰ Medical Discoveries, 2010, Dental Drill.
- ⁴¹ H. C. Altinoz et al., A pilot study of measurement of the frequency of sounds emitted by high-speed dental air turbines, *Journal of Oral Science*, **43**, Issue 3, 2001, pp. 189-192.
- ⁴² C. Forster, *Musical Mathematics (On the Art and Science of Acoustic Instruments)*, Chronicle Books, San Francisco, 2010, pp. 118-130.
- ⁴³ J. Larmor, On a Dynamical Theory of The Electric and Luminiferous Medium, *Philosophical Transactions of the Royal Society*, **190** (1897), pp. 205–300.
- ⁴⁴ D. F. Gaitan, L. A. Crum, R. A. Roy, C. C. Church. "Sonoluminescence and Bubble Dynamics for a Single, Stable, Cavitation Bubble". *The Journal of the Acoustical Society of America* 91 (6): 3166–3183 (1992).